

---

# Gated Neural Networks for Implied Volatility Surfaces

---

Yu Zheng<sup>♣ ♠ \*</sup>   Yongxin Yang<sup>♣ ◇ †</sup>   Bowei Chen<sup>♡ ‡</sup>

♣ ArrayStream Technologies, London, UK

♠ Department of Finance & Financial Innovation Center, Southwestern University of Finance and Economics, China

◇ School of Informatics, University of Edinburgh, UK

♡ Adam Smith Business School, University of Glasgow, UK

## Abstract

This paper presents a framework of developing neural networks to predict implied volatility surfaces. It can incorporate the related properties from existing mathematical models and empirical findings, including no static arbitrage, limiting boundaries, asymptotic slope and volatility smile. These properties are also satisfied empirically in our experiments with the option data on the S&P 500 index over 20 years. The developed neural network model outperforms the widely used surface stochastic volatility inspired (SSVI) model and other benchmarked neural network models on the mean average percentage error in both in-sample and out-of-sample datasets. This study has two major contributions. First, it contributes to the recent use of machine learning in finance, and an accurate deep learning implied volatility surface prediction model is obtained. Second, it provides the methodological guidance on how to seamlessly combine data-driven models with domain knowledge in the development of machine learning applications.

## 1 Introduction

Technology has been widely used in finance to bring automation and improve efficiency. It includes using mobile devices for online banking, creating new digital assets based on blockchain like cryptocurrency, and developing data-driven algorithms using machine learning (or broadly artificial intelligence) to price financial products or construct investment strategies. All these activities have formed an emerging new multidisciplinary subject called *financial technology* (in short *fintech*), combining the fields of finance, mathematics, computer science, information systems, and operations research [23]. According to a recent report from Ernst and Young [14], the global fintech funding has a compound annual growth rate of 44% from 2013 to 2017. It increased in 2017 with US\$ 12.2 billion in the first three quarters as compared with US\$ 11.7 billion in the first three quarters of 2016. Within fintech, machine learning has become one of the

hottest sectors, with expected direct investment growth of 63% from 2016 to 2022.

This paper discusses an state-of-the-art machine learning application in finance and a neural network model is developed to predict implied volatility surfaces. Implied volatility is an important financial metric that captures the market's view of the likelihood of changes in a given asset price. Technically, an *implied volatility* is defined as the inverse problem of option pricing, mapping from the option price of the asset in the current market to a single value [12]. When it is plotted against the option strike price and the time to maturity, it is called the *implied volatility surface*.

Specifically, we propose an innovative framework of developing neural networks tailored to the unique characteristics of implied volatility surfaces. A new deep neural network architecture is designed based on gate operators where the gates control the contribution of each source to the targeted outputs of the layers. A new activation function is formulated in order to reproduce volatility smile [12], which is a stylised fact<sup>1</sup> of implied volatility. Several mathematical properties related to implied volatility surfaces are also taken into account, including no static arbitrage, boundaries, and asymptotic slope. These properties will be briefly introduced in Theorem 1 when we discuss the model setup. They are properly incorporated into our model in terms of different loss functions. We validate the proposed framework with the option data on the S&P 500 index covering over 20 years. Compared with the related studies, the experimental settings in this paper are more challenging, so the model needs to be more robust and stable. Our model outperforms the widely used financial model and other benchmarked neural networks on the mean average percentage error in both in-sample and out-of-sample datasets. In the meantime, the stylised fact and the mathematical properties of implied volatility surfaces are satisfied empirically in experiments.

Implied volatility surfaces have been widely studied in mathematical finance. A number of related literature will be reviewed in Section 2. To the best of our knowledge, our research is one of the very first studies which discusses the implied volatility surface prediction using deep neural networks. The research of this paper is multidisciplinary. From a high level perspective,

---

\* ✉ zhengyu@swufe.edu.cn

† ✉ yongxin.yang@ed.ac.uk

‡ ✉ bowei.chen@glasgow.ac.uk (corresponding author)

---

<sup>1</sup> A stylised fact is a term used in economics and finance to refer to empirical findings that are so consistent across a wide range of assets, markets and time periods that they are accepted as truth [39].

it contributes to the recent use of machine learning in finance, and we obtain the best performance prediction model for implied volatility surface of the S&P 500 Index options. Technology wise, our study provides a methodological contribution in the development of machine learning applications. Unlike many existing studies, which used machine learning algorithms as a “black box”, we incorporate a significant domain knowledge into model development, including the design, use and setting of network architecture, activation function, and loss function. Therefore, our study bridges the gap between the data-driven machine learning algorithms and the existing financial theories.

The rest of the paper is organised as follows. Section 2 reviews the related literature. Section 3 provides the model setup. Section 4 introduces our network architecture design. Section 5 discusses the model calibration. Section 6 presents our experimental results, and Section 7 concludes the paper.

## 2 Related Work

Our research touches upon two streams of literature: mathematical finance and machine learning. For the former, we introduce the basic concepts of volatility and discuss the important implied volatility models, mainly from mathematical finance. For the latter, we review a number of recent applications of machine learning in finance.

### 2.1 Implied Volatility Models in Mathematical Finance

In 1973, Fischer Black and Myron Scholes proposed an elegant closed-form pricing formula for the European style call options written on financial assets (simply called the *Black-Scholes option pricing model*) [5], where an underlying financial asset price is driven by a geometric Brownian motion [38] containing a drift and a volatility, and the volatility term shows the small fluctuations of asset returns representing risk. The seminal work of Black and Scholes opened the floodgates of studying mathematical models in finance, then latter created a sub-field called *mathematical finance* (sometimes *stochastic finance*), and the volatility models have become popular since then [41, 15].

Mathematical models of implied volatility surfaces can be simply classified into two groups [25]. The first group is called *indirect methods*, in which an implied volatility is driven by another dynamic model such as local volatility models, stochastic volatility models and Lévy models. Notable studies include [35], [24], [30], [9], [27] and [40]. Models in this group usually have a limited number of parameters, and the volatility term is fitted by the market data along with the asset dynamics, e.g., the geometric Brownian motion and the mean-reversion jump-diffusion process. These models exhibit a very high degree of mathematical elegance but are sometimes invalid empirically. Time-dependent parameters can be included but they will greatly increase computational time and optimisation difficulty in model calibration. The second group is called *direct methods*, in which an implied volatility is specified explicitly. Direct methods can also be divided into two major types. The first type specifies the dynamics of an implied volatility surface and assumes it evolves continuously over time [12, 8]. The second

type pays attention to the static representation of implied volatility surfaces. It does not consider the evolution of the underlying asset, but uses either parametric or non-parametric methods to fit an implied volatility surface and then for prediction.

Static models have been widely studied and used by practitioners and academics. One most popular static model is the stochastic volatility inspired (SVI) model proposed by Gatheral [16]. It models the implied volatility slice for a fixed time to maturity. Kotzé et al. then constructed an arbitrage-free implied volatility surface by introducing a quadratic deterministic volatility function, and the arbitrage-free conditions are forced by solving two minimization problems [29]. Gatheral and Jacquier [17] then further updated the SVI model to the surface SVI (in short SSVI) model, which has a simpler representation than the SVI on the no static arbitrage property and has soon been widely adopted by investors. In addition to the above popular models, Itkin [26] proposed a non-parametric method to model implied volatility surfaces using polynomials of sigmoid functions. However, arbitrage-free conditions are held only at the nodes of discrete strike-expiry space. Corlay [13] employed B-splines to construct an arbitrage-free implied volatility surface and proposed a new calibration method tailored to sparse option data. It should further be noted that static models are relevant to our study in this paper. Within the mentioned models, we choose the recent and most widely used SSVI model as the benchmarked financial model, and later compare its performance with our proposed neural network model in experiments.

### 2.2 Applications of Machine Learning in Finance

Applying machine learning in finance can go back more than a decade earlier, to the late 1980’s or early 1990’s. Pau [36] summarised some of the fundamental challenges which the financial industry puts onto decision making and described a number of attempts such as knowledge based-systems, natural language interfaces, and information screens. Malliaris and Salchenberger [33] demonstrated that a single hidden layer neural network can offer a valuable alternative to estimating option prices to the Black-Scholes model. Malliaris and Salchenberger [34] then used several single hidden layer neural networks to forecast the future volatility of the S&P 100 index. Harrald and Kamstra [22] described a neural network approach which evolves single hidden-layer perceptrons to combine forecasts of stock price volatility, demonstrating the utility of evolutionary programming in a concrete application. Suzuki et al. [42] proposed an agent-based prospect theoretical model and demonstrated that the loss-aversion feature of investors is capable of explaining the financial stylised facts – implied volatility smile and skewness premium. Gavrishchaka [18] proposed a boosting-based framework for volatility prediction in which a collection of generalized autoregressive conditional heteroskedasticity models are trained separately and then combined to form a strong predictor. This approach is also called *ensemble learning*. Weissensteiner [44] used a Q-learning approach to maximize the expected utility of consumption for strategic asset allocation decisions of an investor with a finite planning horizon. Audrino and Colangelo [3] presented a semi-parametric method for predicting implied volatility surfaces in which the base model is a

regression tree and the difference between the model prediction and the actual value is sequentially minimised by adding more trees. Coleman et al. [11] used kernel machines [43] to calibrate the volatility function for option pricing. Wu et al. [45] developed a new sentiment ontology to conduct context-sensitive sentiment analysis of online opinion posts in stock markets. Their methodology can integrate popular sentiment analysis into machine learning approaches based on support vector machine and generalized autoregressive conditional heteroskedasticity modelling. The above mentioned studies have shown great success of applying machine learning into finance which provide alternative solutions to stochastic finance models.

Recently, Yang et al. [46] proposed a class of gated neural networks that can automatically learn to divide-and-conquer the problem space [20] for robust and accurate pricing European options. Inspired by their work, we develop a gated neural network to predict implied volatility surfaces in this paper. Our network architecture is similar to Yang et al. [46]. However, the research in this paper is significantly different from theirs in four important aspects. First, we focus on implied volatility surface prediction while Yang et al. [46] investigated option pricing. Second, we propose an innovative activation function to reflect the stylised fact volatility smile. Third, several mathematical properties related to implied volatility surfaces such as no static arbitrage, limiting boundaries, asymptotic slope, are included into our model development and training. Fourth, our analysis in experiments examines more dimensions. For example, we do not only investigate the implied volatility surface predictions but also the option price predictions if we use the predicted volatilities in the Black-Scholes model. The empirical and mathematical properties related to implied volatility surfaces are also examined.

### 3 Model Setup

Let  $(S_t)_{t \geq 0}$  be the spot price of an asset at time  $t$ , defined on a filtered probability space  $(\Omega, \mathcal{F}, (\mathcal{F}_t)_{t \geq 0}, \mathbb{P})$ , where  $\Omega$  is the sample space,  $\mathcal{F}$  is a sigma-field,  $(\mathcal{F}_t)_{t \geq 0}$  is a filtration and  $\mathbb{P}$  is the probability space. The market is assumed to be arbitrage-free and the time to maturity of a financial product is always finite. To avoid dealing with interest rates and dividends, the forward measure can be used [12]. Let  $(F_{t,T})_{t \geq 0}$  be the forward price of the asset with maturity date  $T$ . It can be calculated by  $\frac{S_t}{B(t,T)}$  where  $B(t,T)$  is the price at time  $t$  of a zero-coupon bond paying one unit at time  $T$ . The no-arbitrage assumption ensures there exists an equivalent martingale measure in which  $(F_{t,T})_{t \geq 0}$  is a martingale [12]. The log forward moneyness  $m$  can be obtained by  $\log\{\frac{K}{F_{t,T}}\}$ , where  $K$  is the strike price. The annualized time to maturity  $\tau$  is then defined as  $\frac{T-t}{A}$ , where  $A$  is the annualization factor. Therefore, the implied volatility  $v(m, \tau)$  can be rewritten as a function of  $m$  and  $\tau$ , and its ground truth value can be obtained by inverting the BlackScholes option pricing formula.

Implied volatility surfaces have been well studied in financial literature. Three important mathematical properties should be taken into account: absence of arbitrage [21]; limiting boundaries [7]; and asymptotic slope [31]. In order to have a conve-

nient mathematical representation, these properties are decomposed into eight conditions and are summarised in Theorem 1. Specifically, conditions 1-5 ensure the absence of arbitrage, conditions 6-7 specify the limiting boundaries, and condition 8 is the asymptotic slope.

**Theorem 1** Let  $d_{\pm}(m, \tau) = -\frac{m}{\sqrt{\tau}v(m, \tau)} \pm \frac{1}{2}\sqrt{\tau}v(m, \tau)$ ,  $n(\cdot)$  be the probability density function of a standard normal distribution, and  $N(\cdot)$  be the cumulative function of a standard normal distribution. The following conditions should hold for an implied volatility surface  $v(m, \tau)$ :

1. **(Positivity)** For  $(m, \tau) \in \mathbb{R} \times \mathbb{R}^+$ ,  $v(m, \tau) > 0$ .
2. **(Twice Differentiability)** For  $\tau > 0$ ,  $m \rightarrow v(m, \tau)$  is twice differentiable on  $\mathbb{R}$ .
3. **(Monotonicity)** For  $m \in \mathbb{R}$ ,  $\tau \rightarrow \sqrt{\tau}v(m, \tau)$  is increasing on  $\mathbb{R}^+$ , then  $v(m, \tau) + 2\tau\partial_{\tau}v(m, \tau) \geq 0$ .
4. **(Absence of Butterfly Arbitrage)** For  $(m, \tau) \in \mathbb{R} \times \mathbb{R}^+$ ,

$$\left[1 - \frac{m\partial_m v(m, \tau)}{v(m, \tau)}\right]^2 - \frac{1}{4}[v(m, \tau)\tau\partial_m v(m, \tau)]^2 + \tau v(m, \tau)\partial_{mm}v(m, \tau) \geq 0.$$

5. **(Limiting Behaviour)** If  $\tau > 0$ , then

$$\lim_{m \rightarrow +\infty} d_+(m, \tau) = -\infty.$$

6. **(Right Boundary)** If  $m \geq 0$ , then

$$N(d_-(m, \tau)) - \sqrt{\tau}\partial_m v(m, \tau)n(d_-(m, \tau)) \geq 0.$$

7. **(Left Boundary)** If  $m < 0$ , then

$$N(-d_-(m, \tau)) + \sqrt{\tau}\partial_m v(m, \tau)n(d_-(m, \tau)) \geq 0.$$

8. **(Asymptotic Slope)** For  $\tau > 0$ ,  $2|m| - v^2(m, \tau)\tau > 0$ .

In addition to Theorem 1, volatility smile has been considered an important stylised fact, which should be included in our model. For a given time to maturity, when the implied volatility is plotted against the strike price, it creates a line that slopes upward on either end, looking like a ‘‘smile’’. In order to include volatility smile in our model, the following smile function  $\phi(\cdot)$  for the log forward moneyness is defined:

$$\phi(z) = \sqrt{z \tanh(z + \frac{1}{2}) + \tanh(-\frac{1}{2}z + \epsilon)}, \quad z \in \mathbb{R}, \quad (1)$$

where  $\tanh(\cdot)$  is the hyperbolic tangent function and  $\epsilon$  is a small value to ensure numerical stability. The function exhibits not only a skew pattern like volatility smile but also meets the second condition of Theorem 1 as it is smoothly twice differentiable with the co-domain  $(0, \infty)$ .

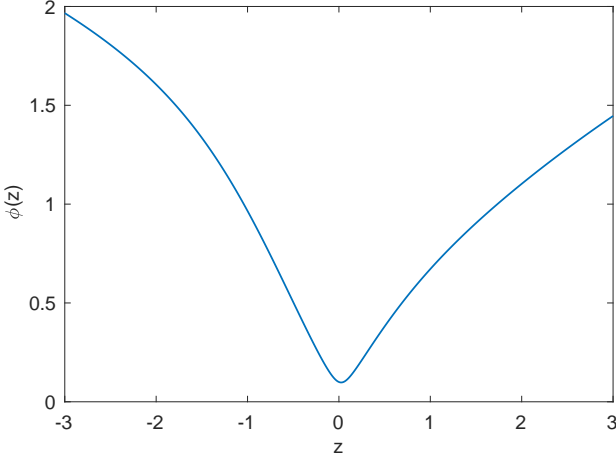


Figure 1: Plot of the smile function  $\phi(\cdot)$  where  $\epsilon = 0.01$ .

## 4 Architecture Design

Fig. 2 presents a schematic view of our neural network architecture design. Our model is called the *multi-model* because it uses several single models as building blocks and their weights are specified by another neural network. The input of the multi-model is the log forward moneyness  $m$  and the time to maturity  $\tau$ ; and the output is the predicted implied volatility  $\hat{v}(m, \tau)$ . Simply, a neural network is based on a collection of connected units called *neurons*. Each connection can transmit a signal from one neuron to another. In our design, additional arithmetic operations on signal transmission are performed at some stages in terms of gate operators. For example,  $\otimes$  is the multiplication gate operator that multiplies the signals it receives, and  $\oplus$  is the addition gate operator, which sums up the signals it receives. For the reader's convenience, a brief description of model parameters is given in Table 1.

As depicted in Fig. 2, each single model can be used to model an implied volatility surface. Mathematically, a single model can be expressed as follows:

$$\begin{aligned} \hat{v}(m, \tau) &= y(m, \tau) \\ &= \sum_{j=1}^J \phi(m\bar{W}_{1,j} + \bar{b}_j) \psi(\tau\bar{W}_{1,j} + \bar{b}_j) e^{\hat{W}_{j,1}} + e^{\hat{b}}, \end{aligned} \quad (2)$$

where  $\phi(\cdot)$  is the smile function to activate neurons related to  $m$  and  $\psi(\cdot)$  is the sigmoid function to activate neurons related to  $\tau$ ,  $J$  is the number of neurons in the hidden layer, and  $\bar{b}$ ,  $\bar{W}$ ,  $\hat{b}$ ,  $\bar{W}$ ,  $\hat{W}$ ,  $\hat{b}$  are network parameters. Each of  $\bar{b}$ ,  $\bar{W}$ ,  $\hat{b}$ ,  $\bar{W}$ ,  $\hat{W}$  has  $J$  elements and  $\hat{b}$  has one element. Therefore, there is a total of  $5J + 1$  parameter values. It should be noted that the predicted implied volatility from Eq. (2) is always positive, satisfying the first condition of Theorem 1.

Single models are used as building blocks and are combined to construct a deeper and more complex architecture. The multi-

model can be expressed as follows:

$$\hat{v}(m, \tau) = \sum_{i=1}^I y_i(m, \tau) w_i(m, \tau), \quad (3)$$

$$y_i(m, \tau) = \sum_{j=1}^J \phi(m\bar{W}_{1,j}^{(i)} + \bar{b}_j^{(i)}) \psi(\tau\bar{W}_{1,j}^{(i)} + \bar{b}_j^{(i)}) e^{\hat{W}_{j,1}^{(i)}} + e^{\hat{b}^{(i)}}, \quad (4)$$

$$w_i(m, \tau) = \frac{e^{\sum_{k=1}^K \psi(m\hat{W}_{1,k} + \tau\hat{W}_{2,k} + \hat{b}_k) \hat{W}_{k,i} + \hat{b}_i}}{\sum_{i=1}^I e^{\sum_{k=1}^K \psi(m\hat{W}_{1,k} + \tau\hat{W}_{2,k} + \hat{b}_k) \hat{W}_{k,i} + \hat{b}_i}}, \quad (5)$$

where  $\hat{W}$ ,  $\hat{b}$ ,  $\hat{W}$ ,  $\hat{b}$  are the newly added parameter terms of the network for weighting single models. The dimensions of  $\hat{W}$ ,  $\hat{b}$ ,  $\hat{W}$ ,  $\hat{b}$  are  $2 \times K$ ,  $K \times 1$ ,  $K \times I$ , and  $I \times 1$ , respectively. Therefore, the total number of parameter values in the multi-model is  $(5J + K + 2)I + 3K$ .

## 5 Optimisation

The designed neural network needs to be calibrated with the market data so that it can be used for prediction. The aim is to minimise the in-sample difference between the predicted  $\hat{v}$  and the ground truth  $v$ . Mathematically, the model training can be expressed by minimising the following loss function  $\ell$ :

$$\ell = \ell_0 + \gamma\ell_1 + \delta\ell_2 + \eta\ell_3 + \rho\ell_4 + \omega\ell_5, \quad (6)$$

where  $\ell_0$  is the data loss function,  $\ell_1, \dots, \ell_4$  are the loss functions that incorporate financial conditions discussed in Theorem 1,  $\ell_5$  is the regularization term to avoid over-fitting, and  $\gamma, \delta, \eta, \rho, \omega$  are the hyper-parameters controlling the weights of  $\ell_1, \dots, \ell_5$ .

The data loss  $\ell_0$  is a joint loss function which combines the Mean Squared Log Error (MSLE) and the Mean Squared Percentage Error (MSPE), defined as follows:

$$\ell_0 = \alpha \left[ \underbrace{\frac{1}{N} \sum_{n=1}^N (\log(v_n) - \log(\hat{v}_n))^2}_{\text{MSLE}} \right] + \beta \left[ \underbrace{\frac{1}{N} \sum_{n=1}^N \left( \frac{v_n - \hat{v}_n}{v_n} \right)^2}_{\text{MSPE}} \right], \quad (7)$$

where  $\alpha$  and  $\beta$  are hyper-parameters. In machine learning, a joint loss is often used to deal with sensitive data or high-dimensional feature spaces [19].

The loss function  $\ell_1$  specifies the monotonicity condition in Theorem 1. Let  $a(m, \tau) := v(m, \tau) + 2\tau\partial_\tau v(m, \tau)$  and the objective of  $\ell_1$  is to push  $a(m, \tau)$  to be non-negative. This can be achieved by randomly sampling  $P$  unique values from the domain of  $m$  and  $Q$  unique values from the domain of  $\tau$ . Therefore,  $\ell_1$  is defined as follows:

$$\ell_1 = \sum_{p=1}^P \sum_{q=1}^Q \max\{0, -a(m_p, \tau_q)\}. \quad (8)$$

It is not difficult to see that  $\ell_1$  adds a penalty if negative values are produced by  $a(m, \tau)$  for a certain set of  $(m, \tau)$  pairs. Therefore, if an infinite number of samples is generated,  $\ell_1$  can be

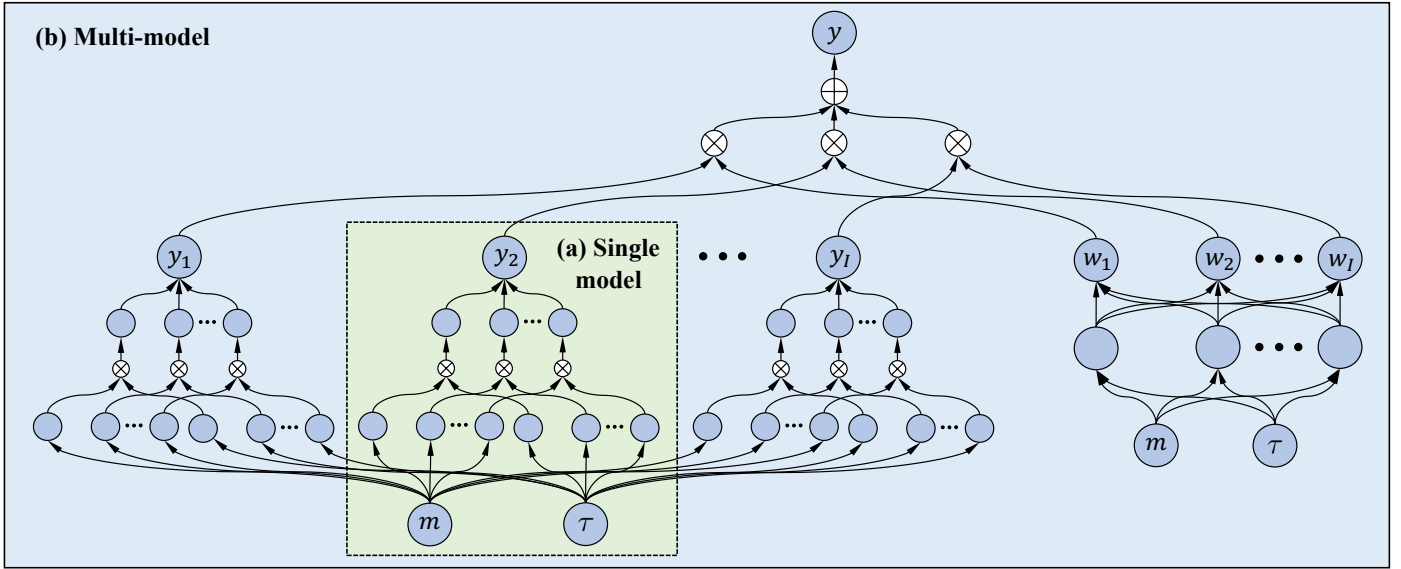


**Figure 2: Schematic view of neural network architecture design: (a) the single model; (b) the multi-model. The multi-model consists of several single models and their weights are given by another neural network. Bias terms are omitted;  $\otimes$  is the multiplication gate operator;  $\oplus$  is the addition gate operator.**

**Table 1: Neural network parameters.**

Notation	Description	Shape	Number in single model	Number in multi-model
$\bar{W}$	Weight term for log forward moneyness	$1 \times J$	1	$I$
$\bar{b}$	Bias term for log forward moneyness	$J \times 1$	1	$I$
$\tilde{W}$	Weight term for time to maturity	$1 \times J$	1	$I$
$\tilde{b}$	Bias term for time to maturity	$J \times 1$	1	$I$
$\hat{W}$	Weight term for final prediction	$J \times 1$	1	$I$
$\hat{b}$	Bias term for final prediction	1	1	$I$
$\dot{W}$	Weight term in the hidden layer for weighting model	$2 \times K$	0	1
$\dot{b}$	Bias term in the hidden layer for weighting model	$K \times 1$	0	1
$\ddot{W}$	Weight term in the output layer for weighting model	$K \times I$	0	1
$\ddot{b}$	Bias term in the output layer for weighting model	$I \times 1$	0	1

reduced to zero during the optimisation and the condition would be met.

The loss function  $\ell_2$  specifies the absence of butterfly arbitrage condition in Theorem 1. Let  $b(m, \tau) := (1 - \frac{m \partial_m v(m, \tau)}{v(m, \tau)})^2 - \frac{(v(m, \tau) \tau \partial_m v(m, \tau))^2}{4} + \tau v(m, \tau) \partial_{mm} v(m, \tau)$  and the objective is to push  $b(m, \tau)$  to be non-negative. This can be achieved using the same way as  $\ell_1$ , by randomly sampling  $P$  unique values from the domain of  $m$  and  $Q$  unique values from the domain of  $\tau$ . Then  $\ell_2$  is defined as follows:

$$\ell_2 = \sum_{p=1}^P \sum_{q=1}^Q \max\{0, -b(m_p, \tau_q)\}. \quad (9)$$

The loss function  $\ell_3$  specifies the left and right boundary conditions in Theorem 1. Let

$$\begin{aligned} c_1(m, \tau) &= N(d_-(m, \tau)) - \sqrt{\tau} \partial_m v(m, \tau) n(d_-(m, \tau)), \\ c_2(m, \tau) &= N(-d_-(m, \tau)) + \sqrt{\tau} \partial_m v(m, \tau) n(d_-(m, \tau)). \end{aligned}$$

The objective of  $\ell_3$  is to push both functions to be non-negative.

To achieve this,  $P_1$  and  $P_2$  unique non-negative values can be sampled from the domain of  $m$ , and  $Q$  unique values from the domain of  $\tau$ . Then  $\ell_3$  is defined as follows:

$$\begin{aligned} \ell_3 &= \sum_{p_1=1}^{P_1} \sum_{q=1}^Q \max\{0, -c_1(m_{p_1}, \tau_q)\} \\ &+ \sum_{p_2=1}^{P_2} \sum_{q=1}^Q \max\{0, -c_2(m_{p_2}, \tau_q)\}. \end{aligned} \quad (10)$$

The loss function  $\ell_4$  specifies the asymptotic condition in Theorem 1. Let  $g(m, \tau) := 2|m| - v^2(m, \tau)\tau$ . Similar to  $\ell_0, \dots, \ell_3$ ,  $P$  unique values can be sampled from the domain of  $m$  and  $Q$  unique values can be sampled from the domain of  $\tau$ . Then  $\ell_4$  is defined as follows:

$$\ell_4 = \sum_{p=1}^P \sum_{q=1}^Q \max\{0, -(g(m_p, \tau_q) - \epsilon)\}, \quad (11)$$

where  $\epsilon = 10^{-5}$  is a small value which ensures  $g(m, \tau)$  to be positive.

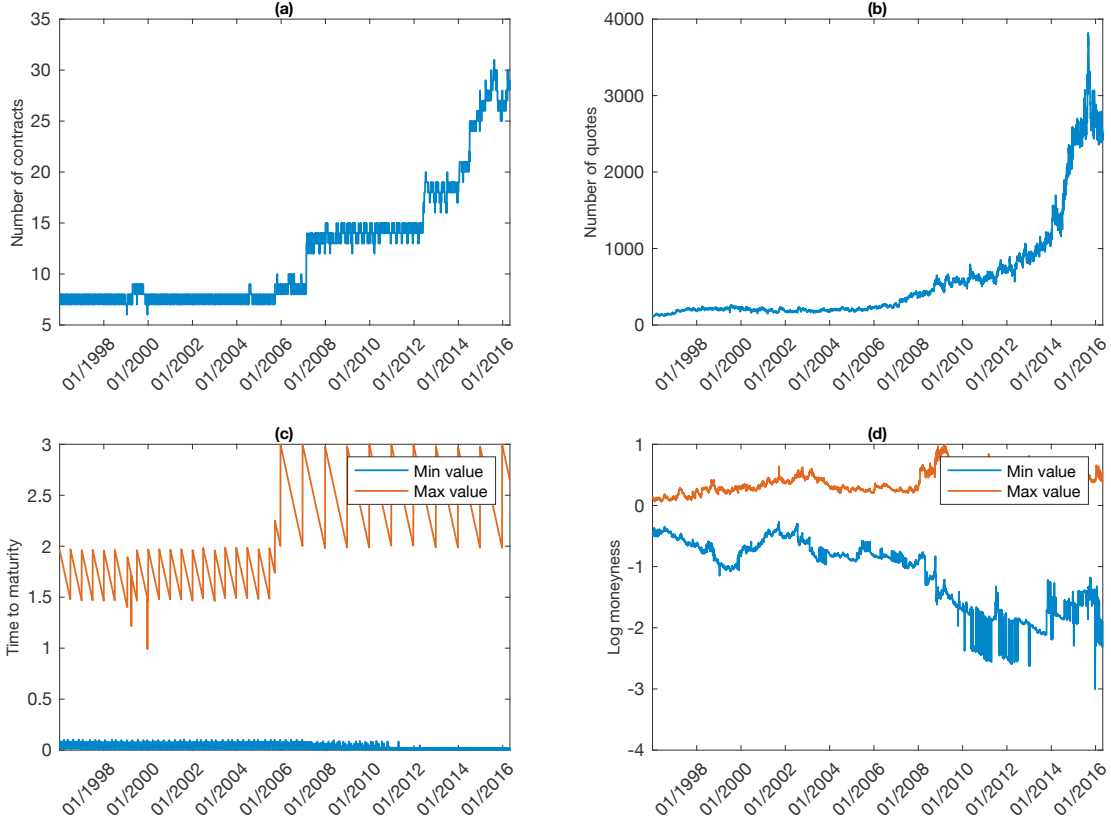


**Figure 3: Time series plots of options from 04/01/1996 to 29/04/2016: (a) the number of contracts; (b) the number of quotes; (c) the time to maturity; (d) the log moneyness.**

To prevent over-fitting, the regularization term  $\ell_5$  is added into the loss function for all weight terms:

$$\ell_5 = \begin{cases} \|\bar{W}\|_F^2 + \|\tilde{W}\|_F^2 + \|\hat{W}\|_F^2, & \text{for the single model,} \\ \sum_{i=1}^I \|\bar{W}^{(i)}\|_F^2 & \text{for the multi-model.} \\ + \sum_{i=1}^I \|\tilde{W}^{(i)}\|_F^2 \\ + \sum_{i=1}^I \|\hat{W}^{(i)}\|_F^2 \\ + \|\dot{W}\|_F^2 + \|\ddot{W}\|_F^2, \end{cases} \quad (12)$$

where  $\|\cdot\|_F^2$  is the square of Frobenius norm, e.g.,  $\|W\|_F^2 = \frac{1}{2} \sum_{i=1}^I \sum_{j=1}^J W_{i,j}^2$ , for an  $I \times J$  weight matrix  $W$ .

It is worth noting that, in Eqs. (8)-(11), we sample  $m$  and  $\tau$  from specific intervals rather than the training data (see Section 6.2 for details). In the practice of machine learning model training, if the training data have limited observations of input variables, creating synthetic data by sampling values from their domains or specific intervals is often used [10, 32]. If their values are sampled from the training data, the calibrated neural network may fail to meet the conditions in the case when their values in prediction are out of the scope of the training data.

## 6 Experiments

In this section, we describe the used option data, introduce the experimental settings, and present our experimental results.

### 6.1 Data

Our option data on the S&P 500 index is obtained from OptionMetrics. It includes a total of 5,116 trading days, covering the period from 04/01/1996 to 29/04/2016. OptionMetrics also provides data on the zero-coupon yield curve, which is constructed based on the London Inter-Bank Offered Rate (LIBOR). However, because the traditional LIBOR-based zero curve is not risk-free after the 2008 financial crisis [1], we extract the Overnight Index Swap (OIS) rates from Bloomberg and bootstrap the zero rate curve from the OIS for the period from 01/01/2008 to 14/10/2016. The zero rate curve provided by OptionMetrics is used for the data prior to 01/01/2008. The risk-free rates are interpolated using a cubic spline to match the option maturity. Forward price is estimated by the put-call parity [4].

### 6.2 Experimental Settings

The original option data is further filtered before model training. Option quotes which are less than  $3/8$  are excluded because they are close to tick size, which might be misleading. The bid-ask mid-point price is calculated as a proxy for the closing price. In-the-money option quotes are excluded because of small transaction volume [6]. Scholars usually do not analyse option contracts with time to maturity of less than 7 days [2]. However, as these options are getting popular recently, e.g., weekly index options, we here analyse option contracts with a short time to maturity and only exclude the contracts with maturity of less

**Table 2: Experimental settings of hyper parameters.**

Parameter	Multi	Multi <sup>†</sup>	Single	Single <sup>†</sup>	Vanilla	Vanilla <sup>†</sup>
$I$	4	4	1	1	1	1
$J$	8	8	32	32	32	32
$K$	5	5	-	-	-	-
Initial learning rate	0.1	0.1	0.1	0.1	0.1	0.1
Number of iterations	20000	20000	20000	20000	20000	20000
$\alpha$	1	1	1	1	1	1
$\beta$	1	1	1	1	1	1
$\gamma$	10	0	10	0	10	0
$\delta$	1	0	1	0	1	0
$\eta$	10	0	10	0	10	0
$\rho$	1	0	1	0	1	0
$\omega$	0.00005	0.00005	0.00005	0.00005	0.00005	0.00005

<sup>†</sup> Model with incomplete constraints.

**Table 3: Mean and standard deviation (Std) of the MAPEs for all models.**

Model	Implied volatility				Option price			
	Training set		Test set		Training set		Test set	
	Mean	Std	Mean	Std	Mean	Std	Mean	Std
Multi	1.74	0.50	3.34	2.18	5.97	1.86	10.64	6.72
Multi <sup>†</sup>	1.76	0.50	3.35	2.17	6.03	1.86	10.67	6.70
Single	2.15	0.67	3.60	2.12	7.38	2.57	11.64	6.68
Single <sup>†</sup>	1.82	0.52	3.38	2.16	6.20	1.91	10.77	6.67
Vanilla	3.21	0.98	4.46	2.07	11.31	3.57	14.61	6.42
Vanilla <sup>†</sup>	2.87	0.80	4.18	2.04	10.53	3.34	14.17	6.60
SSVI	2.59	0.85	3.73	2.18	8.71	2.72	12.74	6.74

<sup>†</sup> Model with incomplete constraints

than 2 days. Analysing options with a short time to maturity is challenging because it requires a model with high robustness and stability. Our prepared data finally contains 63,338 option contracts with 2,986,754 valid quotes. The quotes are then used to calculate implied volatility values by inverting the BlackScholes option pricing formula.

Fig. 3 provides a descriptive summary of the prepared data. As shown in Fig. 3(a), the number of option contracts doubled from 2007 to 2012, and it reached more than 30 contracts for each day in 2016. Therefore, in Fig. 3(b), the number of quotes increases exponentially. Fig. 3(c)(d) present the range of the time to maturity and the log moneyness, which are  $[1, 3]$  and  $[-3, 1]$ , respectively.

Our model is the multi-model. It is compared with the single model and the SSVI for the benchmark. We also compare it with a neural network with the simplest architecture, which has a single hidden layer using the sigmoid activation function and only one constraint that ensures positive output. For simplicity, we call it the *vanilla model*. In addition, to justify the importance of embedding financial conditions in the constrained optimisation, all neural network models are further trained under a setting where  $\ell_1, \dots, \ell_4$  are removed from the loss function in Eq. (6), called the *incomplete constraints* setting. Finally, seven models are examined in experiments, including six different versions of neural networks, the hyper-parameter settings of which

are summarised in Table 2. To avoid the effect of model size on model performance, neural networks with the same architecture design are specified with the same model size. Synthetic data are generated to meet the constraints specified by Eqs. (8)-(11). The ratio of real market data and synthetic data is 1/6.  $m$  is sampled in  $[-6, -3] \cup [3, 6]$  for the asymptotic condition and in  $[-3, 3]$  for other conditions;  $\tau$  is sampled in  $[0.002, 3]$ . These values are set based on the observations from historical data, as shown in Fig. 3 (c)(d).

### 6.3 Results

Neural network models are trained using TensorFlow in Python [37] and we use the method proposed by Kingma and Ba [28] for stochastic optimisation. The selected option quotes available on each trading day are used to compute the mean average percentage error (MAPE) of implied volatilities. The latter can be used to compute option prices; therefore, the MAPE of option prices can be obtained. In the following, we compare our proposed model with the benchmarked models, check if the financial conditions are satisfied, and then investigate the effects of constraints in the optimisation.

Table 3 provides an overall summary of the mean and the standard deviation of MAPEs of implied volatility and option price for each examined model. Our proposed multi-model outperforms other models: (i) on both implied volatility and option

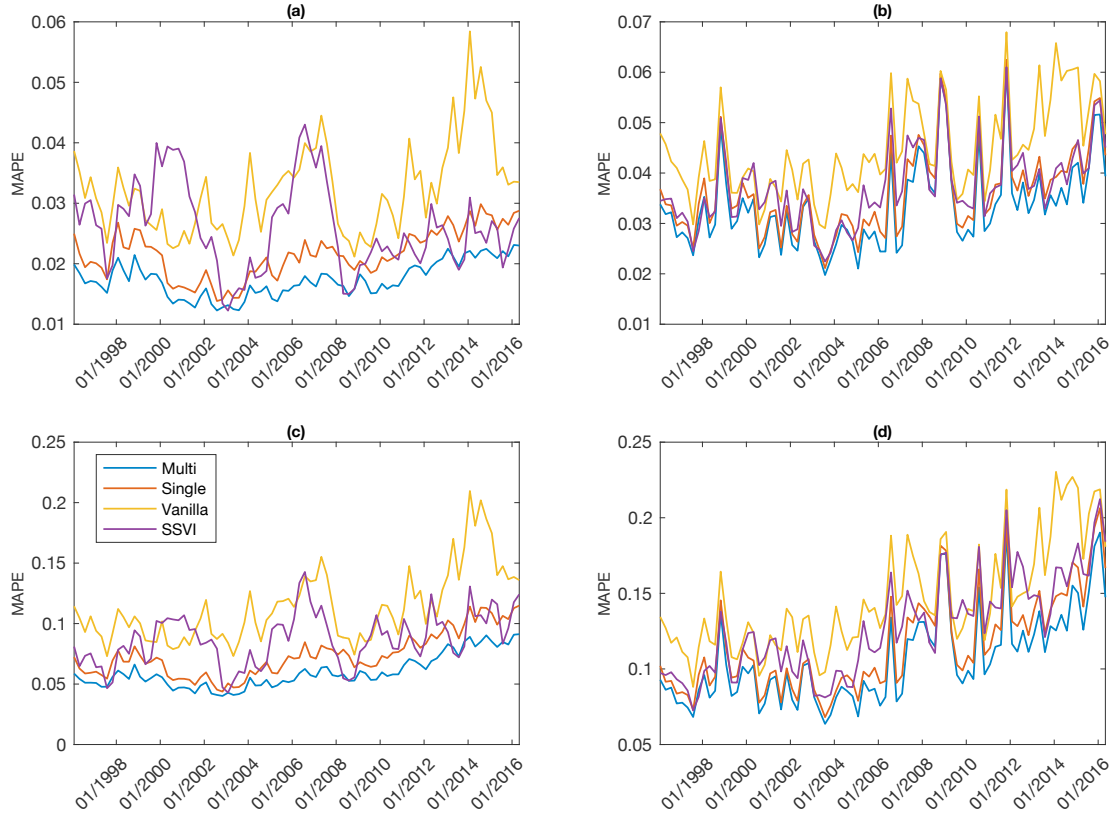


**Figure 4: Plots of the MAPEs in each quarter for the neural network models and the SSVI of: (a) implied volatilities in the training set; (b) implied volatilities in the test set; (c) option prices in the training set; (d) option prices in the test set.**

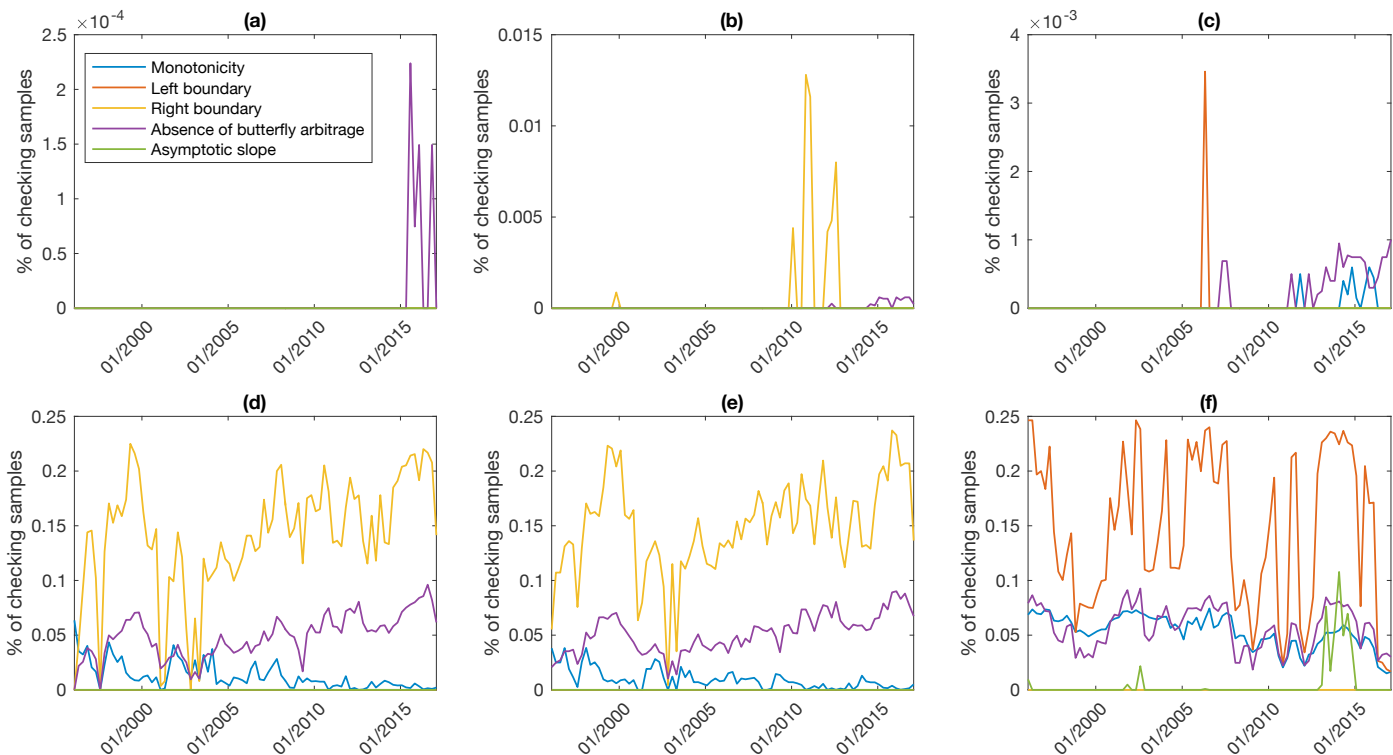
price; and (ii) in both training and test sets. The training set result shows the in-sample error representing how good the model fits the data in calibration, while the test set result shows the out-of-sample error representing the prediction power of the model. Except for vanilla models, other neural network models achieve better performance than the widely used SSVI, affirming that our network architecture design has a great advantage of modelling implied volatility surfaces. Models with incomplete constraints are slightly behind the models with full constraints. Fig. 4 further plots the MAPEs of each quarter to compare the (complete) models with the SSVI in both training and test sets. The multi-model can dynamically capture the data patterns and has the smallest and the most stable moving MAPE over time.

Fig. 5 checks whether the financial conditions set in Theorem 1 are satisfied by neural network models over time, including monotonicity, left boundary, right boundary, absence of arbitrage and asymptotic slope. These conditions are met by the multi-model because the violation percentages are less than 0.1%. Overall, the complete models are more robust than models with incomplete constraints. This justifies the importance of incorporating financial conditions. Figs. 6-7 show why regularization is needed, check if the limit condition is met and compare the implied volatility surface from the multi-model and the multi-model without regularization. As described earlier, regularization is usually used to avoid over-fitting [19], and we can see that the implied volatility surface generated by the multi-model without regularization is not smooth with the “smile” pattern. Fig. 7 further plots the risk-neutral density extracted

from the multi-model and the multi-model without regularization for the forward returns with 11, 32, 109 and 704 days duration. The densities of the forward returns with 109 and 704 days in the multi-model without regularization look strangely like a Gaussian mixture model. The limit condition is also verified by Fig. 7(c).

## 7 Conclusion

In this paper, a gated neural network model is developed to predict implied volatility surfaces. Unlike many previous studies where machine learning techniques were mainly used as a “black box” or were less connected with the existing financial theories, our model has taken into account the related important financial conditions and empirical evidence. To the best of our knowledge, this is one of the very first studies which discuss a methodological framework that can integrate the data-driven machine learning algorithms (particularly deep neural networks) with the existing financial theories. The proposed model framework can be easily extended and applied to solve other similar business problems. In addition to methodological contributions, we validate the proposed model empirically with the option data on the S&P 500 index. Compared with the existing studies, our experimental settings are more challenging because the used option data is over 20 years and the options with a short time to maturity are examined. Therefore, our model needs to be robust in order to produce convincing results. As presented in Section 6, the conventional financial conditions and empirical evidence are



**Figure 5: Plots of condition checks of: (a) the multi-model; (b) the single model; (c) the vanilla model; (d) the multi-model with incomplete constraints; (e) the single model with incomplete constraints; (f) the vanilla model with incomplete constraints.**

met empirically; our model outperforms the widely used SSVI model; and it also outperforms its simplified variations – other similar neural network models without incorporating financial conditions and empirical evidence. The last point also justifies the importance of integrating domain knowledge into the model.

## Acknowledgement

This work was conducted with the support of the UK Economic and Social Research Council through the Impact Acceleration Accounts Business Booster Funding. The first author acknowledges the Imperial College London with the support of the high performance computing equipment for experiments during his PhD study [47]. The authors would also like to thank anonymous reviewers for their helpful comments on earlier drafts of the manuscript.

## References

- [1] F. Ametrano and M. Bianchetti. Everything you always wanted to know about multiple interest rate curve bootstrapping but were afraid to ask. SSRN, 2013. [https://papers.ssrn.com/sol3/papers.cfm?abstract\\_id=2219548](https://papers.ssrn.com/sol3/papers.cfm?abstract_id=2219548).
- [2] T. Andersen, N. Fusari, and V. Todorov. Short-term market risks implied by weekly options. *Journal of Finance*, 72(3):1335–1386, 2017.
- [3] F. Audrino and D. Colangelo. Semi-parametric forecasts of the implied volatility surface using regression trees. *Statistics and Computing*, 20(4):421–434, 2010.
- [4] J. Bilson, S. Kang, and H. Luo. The term structure of implied dividend yields and expected returns. *Economics Letters*, 128:9–13, 2015.
- [5] F. Black and M. Scholes. The pricing of options and corporate liabilities. *Journal of Political Economy*, 81(3):637–654, 1973.
- [6] R. Bliss and N. Panigirtzoglou. Option-implied risk aversion estimates. *Journal of Finance*, 59(1):407–446, 2005.
- [7] P. Carr and L. Wu. Stochastic skew in currency options. *Journal of Financial Economics*, 86(1):213–247, 2007.
- [8] P. Carr and L. Wu. A new simple approach for constructing implied volatility surfaces. SSRN, 2010. [https://papers.ssrn.com/sol3/papers.cfm?abstract\\_id=1701685](https://papers.ssrn.com/sol3/papers.cfm?abstract_id=1701685).
- [9] A. Chockalingam and K. Muthuraman. American options under stochastic volatility. *Operations Research*, 59(4):793–809, 2011.
- [10] J. Choe, S. Park, K. Kim, J. H. Park, D. Kim, and H. Shim. Face generation for low-shot learning using generative adversarial networks. *IEEE International Conference on Computer Vision Workshops*, pages 1940–1948, 2017.

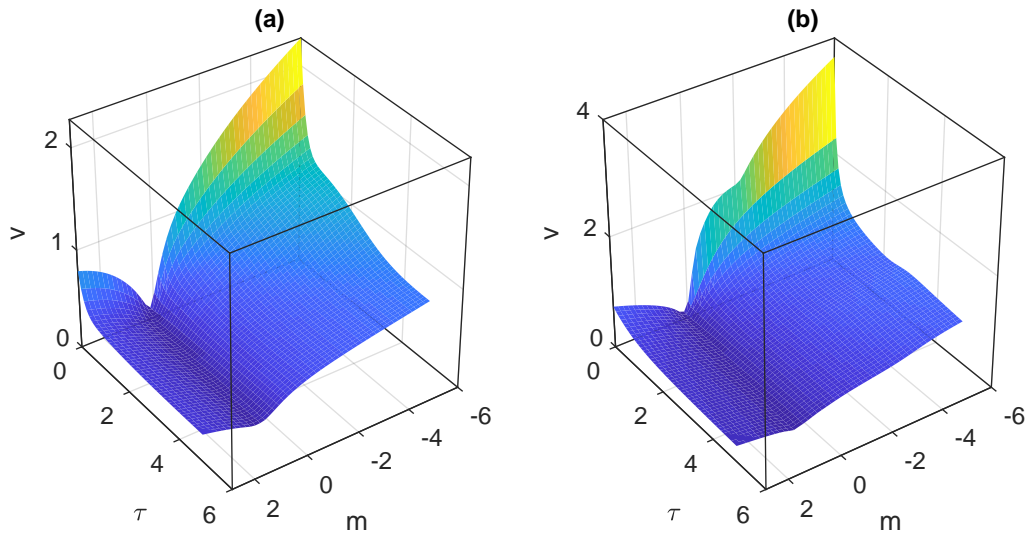


**Figure 6: Plots the implied volatility surface on 11/01/2016 for: (a) the multi-model; and (b) the multi-model without regularization.**

- [11] T. Coleman, Y. Li, and C. Wang. Stable local volatility function calibration using spline kernel. *Computational Optimization and Applications*, 55(3):675–702, 2013.
- [12] R. Cont and J. Da Fonseca. Dynamics of implied volatility surfaces. *Quantitative Finance*, 2(1):45–60, 2002.
- [13] S. Corlay. B-spline techniques for volatility modeling. *Journal of Computational Finance*, 19(3):97–135, 2016.
- [14] Ernst and Young. The future of FinTech and financial services: whats the next big bet? *Technical Report*, 2018.
- [15] P. Friz and J. Gatheral. Valuation of volatility derivatives as an inverse problem. *Quantitative Finance*, 5(6):531–542, 2005.
- [16] J. Gatheral. A parsimonious arbitrage-free implied volatility parameterization with application to the valuation of volatility derivatives. *Presentation at Global Derivatives & Risk Management*, Madrid, 2004.
- [17] J. Gatheral and A. Jacquier. Arbitrage-free svi volatility surfaces. *Quantitative Finance*, 14(1):59–71, 2014.
- [18] V. Gavrishchaka. *Econometric Analysis of Financial and Economic Time Series*, chapter Boosting-based Frameworks in financial modeling: application to symbolic volatility forecasting, pages 123–151. Emerald, 2006.
- [19] I. Goodfellow, Y. Bengio, and A. Courville. *Deep Learning*. MIT Press, 2016.
- [20] N. Gradojevic, R. Gencay, and D. Kukulj. Option pricing with modular neural networks. *IEEE Transactions on Neural Networks*, 20(4):626–637, 2009.
- [21] A. Gulisashvili. *Analytically Tractable Stochastic Stock Price Models*. Springer, 2012.
- [22] P. Harrald and M. Kamstra. Evolving artificial neural networks to combine financial forecasts. *IEEE Transactions on Evolutionary Computation*, 1(1):40–52, 1997.
- [23] T. Hendershott, M. Zhang, L. Zhao, and E. Zheng. Special issue of information systems research fintech innovating the financial industry through emerging information technologies. *Information Systems Research*, 28(4):885–886, 2017.
- [24] S. Heston. A closed-form solution for options with stochastic volatility with applications to bond and currency options. *Review of Financial Studies*, 6(2):327–343, 1993.
- [25] C. Homescu. Implied volatility surface: construction methodologies and characteristics. arXiv, 2011. <https://arxiv.org/abs/1107.1834>.
- [26] A. Itkin. To sigmoid-based functional description of the volatility smile. *The North American Journal of Economics and Finance*, 31:264–291, 2015.
- [27] C. Kang, W. Kang, and J. Lee. Exact simulation of the Wishart multidimensional stochastic volatility model. *Operations Research*, 65(5):1190–1206, 2017.
- [28] D. Kingma and J. Ba. Adam: a method for stochastic optimization. *International Conference on Learning Representations*, pages 1–13, 2015.
- [29] A. Kotzé, C. Labuschagne, M. Nair, and N. Padayachi. Arbitrage-free implied volatility surfaces for options on single stock futures. *The North American Journal of Economics and Finance*, 26:380–399, 2013.
- [30] S. Kou. A jump-diffusion model for option pricing. *Management Science*, 48(8):1086–1101, 2002.
- [31] R. Lee. The moment formula for implied volatility at extreme strikes. *Mathematical Finance*, 14(3):469–480, 2004.

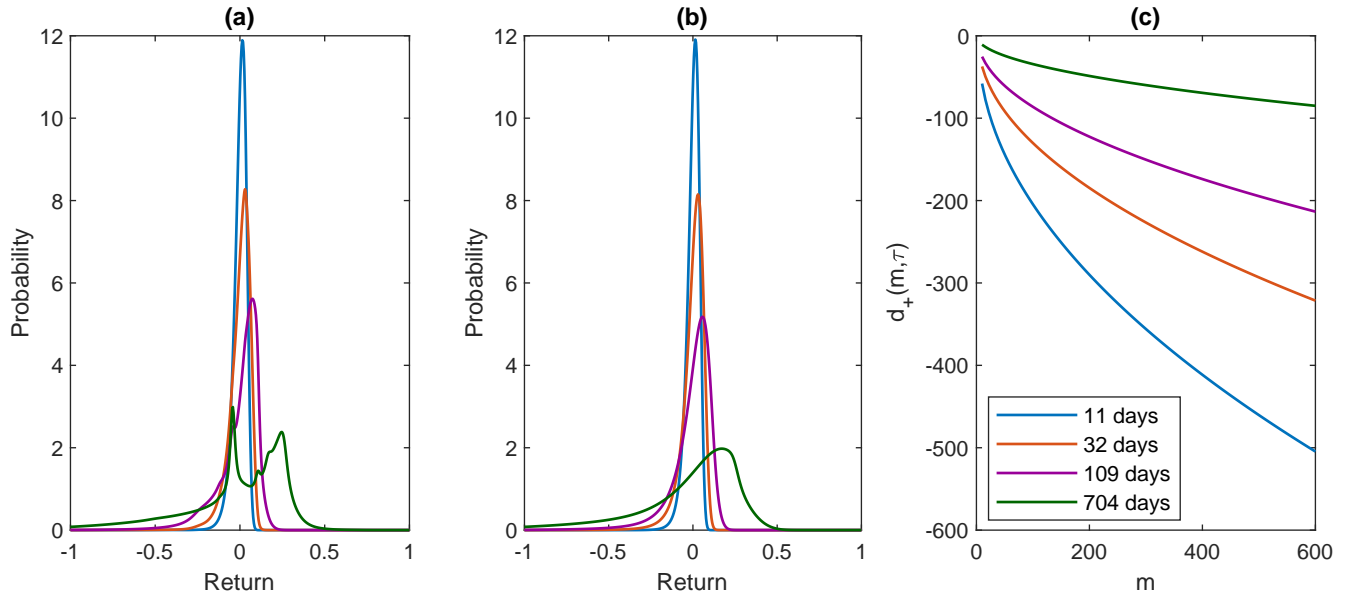


**Figure 7: Plots for the forward with 11, 32, 109 and 704 days duration: (a) the density of returns from the multi-model without regularization; (b) the density of returns from the multi-model; and (c) the limit condition  $d_+(m, \tau)$  in Theorem 1 for the multi-model on 11/01/2016.**

- [32] T. Liu, Y. Cui, Q. Yin, W. Zhang, S. Wang, and G. Hu. Generating and exploiting large-scale pseudo training data for zero pronoun resolution. *Proceedings of the 55th Annual Meeting of the Association for Computational Linguistics*, pages 102–111, 2017.
- [33] M. Malliaris and L. Salchenberger. A neural network model for estimating option prices. *Applied Intelligence*, 3(3):193–206, 1993.
- [34] M. Malliaris and L. Salchenberger. Using neural networks to forecast the S&P 100 implied volatility. *Neurocomputing*, 10(2):183–195, 1996.
- [35] R. Merton. Option pricing when underlying stock returns are discontinuous. *Journal of Financial Economics*, 3:125–144, 1976.
- [36] L. Pau. Artificial intelligence and financial services. *IEEE Transactions on Knowledge and Data Engineering*, 3(2):137–148, 1991.
- [37] A. Roy, S. Qureshi, K. Pande, D. Nair, K. Gairola, P. Jain, S. Singh, K. Sharma, A. Jagadale, Y.-Y. Lin, S. Sharma, R. Gotety, Y. Zhang, J. Tang, T. Mehta, H. Sindhanuru, N. Okafor, S. Das, C. Gopal, S. Rudraraju, and A. Kakarlapudi. Performance comparison of machine learning platforms. *INFORMS Journal on Computing*, 31(2):207225, 2019.
- [38] P. Samuelson. Proof that properly anticipated prices fluctuate randomly. *Industrial Management Review*, pages 41–49, 1965.
- [39] M. Sewell. Characterization of financial time series. Research Note, University College London, 2011.
- [40] K. Shiraya and A. Takahashi. Pricing average and spread options under local-stochastic volatility jump-diffusion models. *Mathematics of Operations Research*, 4(11), 2018.
- [41] S. Sundaresan. Continuous-time methods in finance: a review and an assessment. *Journal of Finance*, 13(4):1057–1099, 2000.
- [42] K. Suzuki, T. Shimokawa, and T. Misawa. Agent-based approach to option pricing anomalies. *IEEE Transactions on Evolutionary Computation*, 13(5):959–972, 2009.
- [43] V. Vapnik. *The Nature of Statistical Learning Theory*. Springer, 2nd edition, 2000.
- [44] A. Weissensteiner. A Q-learning approach to derive optimal consumption and investment strategy. *IEEE Transactions on Neural Networks*, 20(8):1234–1243, 2009.
- [45] D. Wu, L. Zheng, and D. Olson. A decision support approach for online stock forum sentiment analysis. *IEEE Transactions on Systems, Man, and Cybernetics: Systems*, 44(8):1077–1087, 2014.
- [46] Y. Yang, Y. Zheng, and T. Hospedales. Gated neural networks for option pricing: rationality by design. *Proceedings of the Thirty-First AAAI Conference on Artificial Intelligence*, 2017.
- [47] Y. Zheng. *Machine Learning and Option Implied Information*. PhD thesis, Imperial College London, 2018.